

Preparation of Microcrystalline $\text{NaSrY}(\text{MoO}_4)_3$: $\text{Eu}^{3+}/\text{Yb}^{3+}$ Phosphors via Microwave Sol-Gel Route and their Spectroscopic Properties

Chang Sung Lim

Department of Advanced Materials Science & Engineering, Hanseo University, Seosan 356-706
Republic of Korea

Abstract: $\text{NaSrY}_{1-x}(\text{MoO}_4)_3$: $\text{Eu}^{3+}/\text{Yb}^{3+}$ phosphors with doping concentrations of Eu^{3+} and Yb^{3+} ($x = \text{Eu}^{3+} + \text{Yb}^{3+}$, $\text{Eu}^{3+} = 0.05, 0.1, 0.2$ and $\text{Yb}^{3+} = 0.2, 0.45$) were successfully synthesized via microwave sol-gel route; their spectroscopic properties were investigated. Well-crystallized particles showed a fine and homogeneous morphology with particle sizes of 2-5 μm . Under excitation at 980 nm, $\text{NaSrY}_{0.5}(\text{MoO}_4)_3$: $\text{Eu}_{0.05}\text{Yb}_{0.45}$ particles exhibited a very strong 475-nm emission band in the blue region, and a strong 525-nm and a weak 550-nm emission bands in the blue region, while a very weak 650-nm emission band in the red region. The Raman spectra of the doped particles indicated the domination of strong peaks at higher frequencies of 774, 884, 1364 and 1440 cm^{-1} and the weak peaks at lower frequencies of 324 and 400 cm^{-1} . The highly modulated structure of the doped samples were attributed to the strong mixing of stretching vibrations between the Mo-O bonds and the MoO_4 as well as the quenching effect of Eu^{3+} concentrations.

Key words: $\text{NaSrY}_{1-x}(\text{MoO}_4)_3$: $\text{Eu}^{3+}/\text{Yb}^{3+}$, Microwave sol-gel, Upconversion photoluminescence, Raman spectroscopy.

Introduction

Ln-doped upconversion (UC) particles can be used for a wide range of biomedical applications such as bio-detection, cancer therapy, bio-labeling, fluorescence imaging, magnetic resonance imaging and drug delivery [1-3]. Recently, double molybdate compounds of $\text{MR}_2(\text{MoO}_4)_4$ (M: bivalent alkaline earth metal ion, R: trivalent rare earth ion) belong to a group of double alkaline earth lanthanide molybdates. It is possible for the trivalent rare earth ions in the disordered tetragonal-phase to be partially substituted by Eu^{3+} and Yb^{3+} ions, these ions are effectively doped into the crystal lattices of the tetragonal phase due to the similar radii of the trivalent rare-earth ions in R^{3+} , this results in the excellent UC photoluminescence properties [4-6]. Among rare-earth ions, the Eu^{3+} ion is suitable for converting infrared to visible light through the UC process due to its appropriate electronic energy level configuration. Co-doped Yb^{3+} ion and Eu^{3+} ion can

*Corresponding author: cslim@hanseo.ac.kr

remarkably enhance the UC efficiency for the shift from infrared to visible light due to the efficiency of the energy transfer from Yb^{3+} to Eu^{3+} . The Yb^{3+} ion, as a sensitizer, can be effectively excited by an incident light source energy. This energy is transferred to the activator from which radiation can be emitted [7-9].

Several processes have been developed to prepare these rare-earth doped molybdates. For practical application of UC photoluminescence in products such as lasers, three-dimensional displays, light-emitting devices, and biological detectors, features such as the homogeneous UC particle size distribution and morphology need to be well defined. Compared with the usual methods, microwave synthesis has the advantages of a very short reaction time, small-size particles, narrow particle size distribution, and high purity of final polycrystalline samples. Microwave heating is delivered to the material surface by radiant and/or convection heating, which is transferred to the bulk of the material via conduction [10, 11]. The microwave sol-gel process is a cost-effective method that provides high homogeneity and is easy to scale-up, and it is emerging as a viable alternative approach for quick synthesis of high-quality luminescent materials [12, 13]. However, the $\text{NaSrY}_{1-x}(\text{MoO}_4)_3: \text{Eu}^{3+}/\text{Yb}^{3+}$ ternary molybdate phosphors have not been reported up to now. In this concept, the ternary molybdate $\text{NaSrY}(\text{MoO}_4)_3$ phosphors synthesized via the microwave sol-gel route are reported.

In this study, $\text{NaSrY}_{1-x}(\text{MoO}_4)_3: \text{Eu}^{3+}/\text{Yb}^{3+}$ phosphors with doping concentrations of Eu^{3+} and Yb^{3+} ($x = \text{Eu}^{3+} + \text{Yb}^{3+}$, $\text{Eu}^{3+} = 0.05, 0.1, 0.2$ and $\text{Yb}^{3+} = 0.2, 0.45$) phosphors were prepared via the microwave sol-gel route, followed by heat treatment. The synthesized particles were characterized by X-ray diffraction (XRD), scanning electron microscopy (SEM), and energy-dispersive X-ray spectroscopy (EDS). The optical properties were examined comparatively using photoluminescence (PL) emission and Raman spectroscopy.

Experimental

Appropriate stoichiometric amounts of $\text{Na}_2\text{MoO}_4 \cdot 2\text{H}_2\text{O}$ (99%, Sigma-Aldrich, USA), $\text{Sr}(\text{NO}_3)_2$ (99%, Sigma-Aldrich, USA), $\text{Y}(\text{NO}_3)_3 \cdot 6\text{H}_2\text{O}$ (99%, Sigma-Aldrich, USA), $(\text{NH}_4)_6\text{Mo}_7\text{O}_{24} \cdot 4\text{H}_2\text{O}$ (99%, Alfa Aesar, USA), $\text{Eu}(\text{NO}_3)_3 \cdot 5\text{H}_2\text{O}$ (99.9%, Sigma-Aldrich, USA), $\text{Yb}(\text{NO}_3)_3 \cdot 5\text{H}_2\text{O}$ (99.9%, Sigma-Aldrich, USA), citric acid (99.5%, Daejung Chemicals, Korea), NH_4OH (A.R.), ethylene glycol (A.R.) and distilled water were used to prepare $\text{NaSrY}(\text{MoO}_4)_3$, $\text{NaSrY}_{0.8}(\text{MoO}_4)_3: \text{Eu}_{0.2}$, $\text{NaSrY}_{0.7}(\text{MoO}_4)_3: \text{Eu}_{0.1}\text{Yb}_{0.2}$ and $\text{NaSrY}_{0.5}(\text{MoO}_4)_3: \text{Eu}_{0.05}\text{Yb}_{0.45}$ compounds with doping concentrations of Eu^{3+} and Yb^{3+} ($\text{Eu}^{3+} = 0.05, 0.1, 0.2$ and $\text{Yb}^{3+} = 0.2, 0.45$). To prepare $\text{NaSrY}(\text{MoO}_4)_3$, 0.2 mol% $\text{Na}_2\text{MoO}_4 \cdot 2\text{H}_2\text{O}$ and 0.143 mol% $(\text{NH}_4)_6\text{Mo}_7\text{O}_{24} \cdot 4\text{H}_2\text{O}$ were dissolved in 20 mL of ethylene glycol and 80 mL of 5M NH_4OH under vigorous stirring and heating. Subsequently, 0.4 mol% $\text{Sr}(\text{NO}_3)_2$ and citric acid (with a molar ratio of citric acid to total metal ions of 2:1) were dissolved in 100 mL of distilled water under vigorous stirring and heating. Then, the solutions were mixed together under vigorous stirring and heating at 80-100°C. Finally, highly transparent solutions were obtained and adjusted to pH=7-8 by the addition of NH_4OH or citric acid. In order to prepare $\text{NaSrY}_{0.8}(\text{MoO}_4)_3: \text{Eu}_{0.2}$, the mixture of 0.32 mol% $\text{Y}(\text{NO}_3)_3 \cdot 6\text{H}_2\text{O}$ with 0.08 mol% $\text{Eu}(\text{NO}_3)_3 \cdot 5\text{H}_2\text{O}$ was used for the creation of the rare earth solution. In order to prepare

$\text{NaSrY}_{0.7}(\text{MoO}_4)_3$: $\text{Eu}_{0.1}\text{Yb}_{0.2}$, the mixture of 0.28 mol% $\text{Y}(\text{NO}_3)_3 \cdot 6\text{H}_2\text{O}$ with 0.04 mol% $\text{Eu}(\text{NO}_3)_3 \cdot 5\text{H}_2\text{O}$ and 0.08 mol% $\text{Yb}(\text{NO}_3)_3 \cdot 5\text{H}_2\text{O}$ was used for the creation of the rare earth solution. In order to prepare $\text{NaSrY}_{0.5}(\text{MoO}_4)_3$: $\text{Eu}_{0.05}\text{Yb}_{0.45}$, the rare earth containing solution was generated using 0.2 mol% $\text{Y}(\text{NO}_3)_3 \cdot 6\text{H}_2\text{O}$ with 0.02 mol% $\text{Eu}(\text{NO}_3)_3 \cdot 5\text{H}_2\text{O}$ and 0.18 mol% $\text{Yb}(\text{NO}_3)_3 \cdot 5\text{H}_2\text{O}$.

The transparent solutions were placed for 30 min into a microwave oven operating at a frequency of 2.45 GHz with a maximum output-power of 1250 W. The working cycle of the microwave reaction was controlled very precisely using a regime of 40 s on and 20 s off for 15 min, followed by further treatment of 30 s on and 30 s off for 15 min. The ethylene glycol was evaporated slowly at its boiling point. Ethylene glycol is a polar solvent at its boiling point of 197°C, this solvent is a good candidate for the microwave process. The samples were treated with ultrasonic radiation for 10 min to produce a light yellow transparent sol. After this, the light yellow transparent sols were dried at 120°C in a dry oven to obtain black dried gels. The black dried gels were ground and heat-treated at 900°C for 16 h with 100°C intervals between 600-900°C. Finally, white particles were obtained for $\text{NaSrY}(\text{MoO}_4)_3$ and pink particles were obtained for the doped compositions.

The phase composition of the synthesized particles was identified using XRD (D/MAX 2200, Rigaku, Japan). The microstructure and surface morphology of the doped particles were observed using SEM/EDS (JSM-5600, JEOL, Japan). The PL spectra were

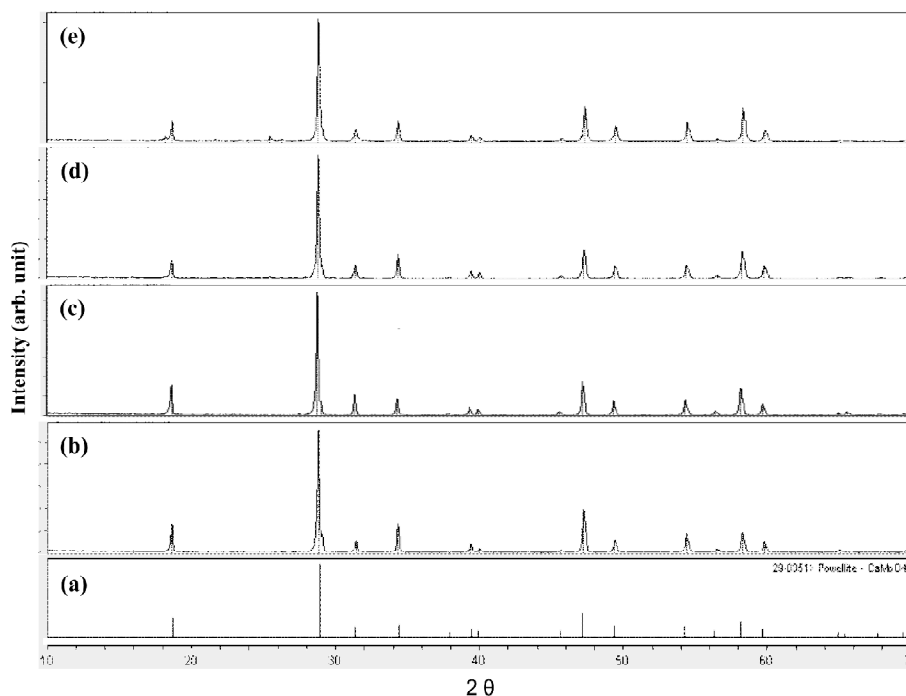


Figure 1: X-ray diffraction patterns of the (a) JCPDS 29-0361 data of CaMoO_4 , and the synthesized (b) $\text{NaSrY}(\text{MoO}_4)_3$, (c) $\text{NaSrY}_{0.8}(\text{MoO}_4)_3$: $\text{Eu}_{0.2}$, (d) $\text{NaSrY}_{0.7}(\text{MoO}_4)_3$: $\text{Eu}_{0.1}\text{Yb}_{0.2}$, and (e) $\text{NaSrY}_{0.5}(\text{MoO}_4)_3$: $\text{Eu}_{0.05}\text{Yb}_{0.45}$ particles.

recorded using a spectrophotometer (Perkin Elmer LS55, UK) at room temperature. Raman spectroscopy measurements were performed using a LabRam Aramis (Horiba Jobin-Yvon, France). The 514.5-nm line of an Ar ion laser was used as the excitation source; the power on the samples was kept at 0.5 mW.

Results and Discussion

Fig. 1 shows the X-ray diffraction patterns of the (a) JCPDS 29-0361 data of CaMoO_4 , and the synthesized (b) $\text{NaSrY}(\text{MoO}_4)_3$, (c) $\text{NaSrY}_{0.8}(\text{MoO}_4)_3:\text{Eu}_{0.2}$, (d) $\text{NaSrY}_{0.7}(\text{MoO}_4)_3:\text{Eu}_{0.1}\text{Yb}_{0.2}$ and (e) $\text{NaSrY}_{0.5}(\text{MoO}_4)_3:\text{Eu}_{0.05}\text{Yb}_{0.45}$ particles. The diffraction patterns of the products can be mostly similar with the standard data of CaMoO_4 (JCPDS 29-0361). No impurity phases were detected. $\text{NaSrY}(\text{MoO}_4)_3$ as a member of ternary molybdate family is tetragonal with a space group $I4_1/a$. In $\text{NaSrY}(\text{MoO}_4)_3$ matrix, Na^+ and Y^{3+} are randomly arranged and form a disordered structure. In the crystal structure of $\text{NaSrY}_{1-x}(\text{MoO}_4)_3$, the Y^{3+} ion site is supposed to be occupied by Eu^{3+} and Yb^{3+} ions with fixed occupations according to the nominal chemical formulas. The defined crystal structure contains MoO_4 tetrahedrons coordinated by four $(\text{Sr}/\text{Na}/\text{Y}/\text{Eu}/\text{Yb})\text{O}_8$ square antiprisms through the common O ions. It is assumed that the radii of Eu^{3+} ($R=1.066 \text{ \AA}$) and Yb^{3+} ($R=0.985 \text{ \AA}$) are similar with Y^{3+} ($R=1.019 \text{ \AA}$), when the coordination number is $\text{CN} = 8$ [14]. Consequently, it should be emphasized that the Eu^{3+} and Yb^{3+} ions can be efficiently doped into the $\text{NaSrY}(\text{MoO}_4)_3$ lattice by partial substitution of Eu^{3+} and Yb^{3+} for Y^{3+} in the Y^{3+} sites, which leads to maintaining the tetragonal structure of the $\text{NaSrY}_{1-x}(\text{Eu},\text{Yb})_x(\text{MoO}_4)_3$. Post heat-treatment plays an important role in reaching of the well-defined crystallized morphology. To reach a well-defined final morphology, the samples need to be heat treated at 900°C for 16 h. It is assumed that the $\text{Eu}^{3+}/\text{Yb}^{3+}$ doping concentrations are acceptable to keep the original structure of $\text{NaSrY}(\text{MoO}_4)_3$.

Fig. 2 provides a SEM image of the synthesized $\text{NaSrY}_{0.50}(\text{MoO}_4)_3:\text{Eu}_{0.05}\text{Yb}_{0.45}$ particles. The as-synthesized samples are well crystallized with a fine and homogeneous morphology and particle size of 2-5 μm . The agglomerated particles are induced by the atom inter-diffusion between the grains. It should be noted that the morphological feature is insensitive to the $\text{Eu}^{3+}/\text{Yb}^{3+}$ doping concentrations. The microwave sol-gel method in application to the ternary molybdate provides the energy to synthesize the bulk of the material uniformly, so that fine particles with controlled morphology can be fabricated in a short time period. The method is a cost-effective way to fabricate highly homogeneous products with easy scale-up and it is a viable alternative for the rapid synthesis of UC particles. This suggests that the microwave sol-gel route is suitable for the creation of homogeneous $\text{NaSrY}_{1-x}(\text{MoO}_4)_3:\text{Eu}^{3+}/\text{Yb}^{3+}$ crystallites.

Fig. 3 shows the energy-dispersive X-ray spectroscopy patterns of the synthesized (a) $\text{NaSrY}_{0.8}(\text{MoO}_4)_3:\text{Eu}_{0.2}$ and (b) $\text{NaSrY}_{0.5}(\text{MoO}_4)_3:\text{Eu}_{0.05}\text{Yb}_{0.45}$ particles, and quantitative compositions of (c) $\text{NaSrY}_{0.8}(\text{MoO}_4)_3:\text{Eu}_{0.2}$ and (d) $\text{NaSrY}_{0.5}(\text{MoO}_4)_3:\text{Eu}_{0.05}\text{Yb}_{0.45}$ particles. The EDS pattern shows that the (a) $\text{NaSrY}_{0.8}(\text{MoO}_4)_3:\text{Eu}_{0.2}$ and (b) $\text{NaSrY}_{0.5}(\text{MoO}_4)_3:\text{Eu}_{0.05}\text{Yb}_{0.45}$ particles are composed of Na, Sr, Y, Mo, O and Eu for $\text{NaSrY}_{0.8}(\text{MoO}_4)_3:\text{Eu}_{0.2}$ and Na, Sr, Y, Mo, O, Eu and Yb for $\text{NaSrY}_{0.5}(\text{MoO}_4)_3:\text{Eu}_{0.05}\text{Yb}_{0.45}$ particles. The quantitative compositions

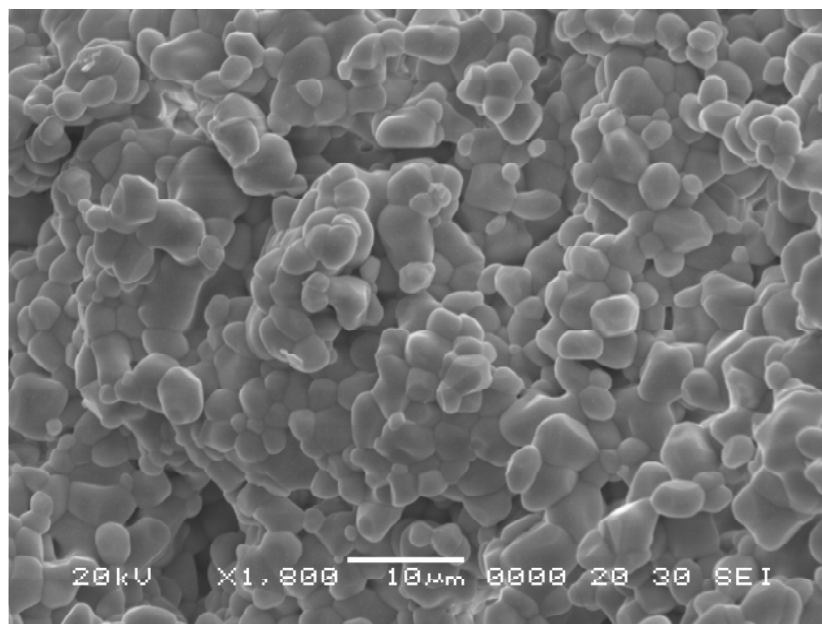


Figure 2: Scanning electron microscopy image of the synthesized $\text{NaSrY}_{0.5}(\text{MoO}_4)_3:\text{Eu}_{0.05}\text{Yb}_{0.45}$ particles.

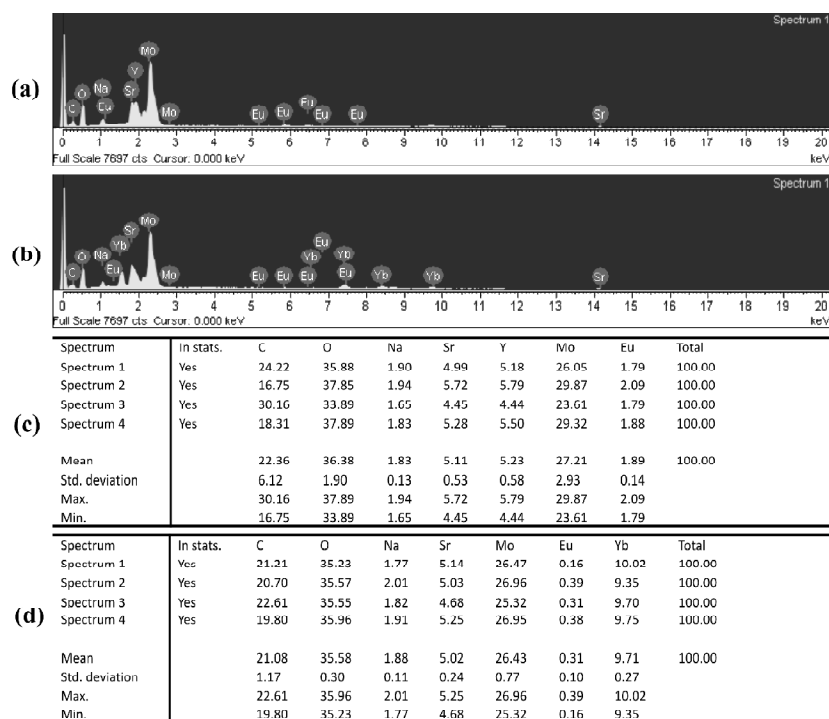


Figure 3: Energy-dispersive X-ray spectroscopy patterns of the synthesized (a) $\text{NaSrY}_{0.8}(\text{MoO}_4)_3:\text{Eu}_{0.2}$ and (b) $\text{NaSrY}_{0.5}(\text{MoO}_4)_3:\text{Eu}_{0.05}\text{Yb}_{0.45}$ particles, and quantitative compositions of (c) $\text{NaSrY}_{0.8}(\text{MoO}_4)_3:\text{Eu}_{0.2}$ and (d) $\text{NaSrY}_{0.5}(\text{MoO}_4)_3:\text{Eu}_{0.05}\text{Yb}_{0.45}$ particles.

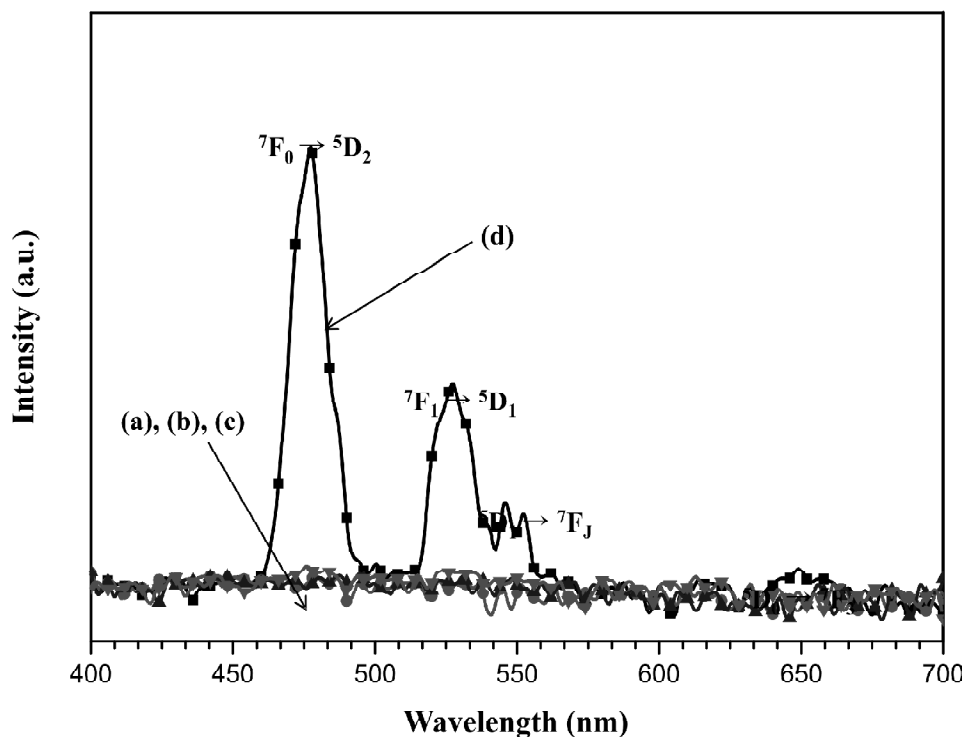


Figure 4: Upconversion photoluminescence emission spectra of (a) $\text{NaSrY}(\text{MoO}_4)_3$, (b) $\text{NaSrY}_{0.8}(\text{MoO}_4)_3:\text{Eu}_{0.2}$, (c) $\text{NaSrY}_{0.7}(\text{MoO}_4)_3:\text{Eu}_{0.1}\text{Yb}_{0.2}$ and (d) $\text{NaSrY}_{0.5}(\text{MoO}_4)_3:\text{Eu}_{0.05}\text{Yb}_{0.45}$ particles excited under 980 nm at room temperature.

of (c) and (d) are in good relation with the nominal compositions of the particles. The relation of Na, Sr, Y, Mo, O, Eu and Yb components provides that $\text{NaSrY}_{0.8}(\text{MoO}_4)_3:\text{Eu}_{0.2}$ and $\text{NaSrY}_{0.5}(\text{MoO}_4)_3:\text{Eu}_{0.05}\text{Yb}_{0.45}$ particles can be successfully synthesized using the microwave sol-gel method. The microwave sol-gel process of ternary molybdate provides the energy to synthesize the bulk of the material uniformly, so that fine particles with controlled morphology can be fabricated in a short time period.

Fig. 4 shows the UC photoluminescence emission spectra of the as-prepared of (a) $\text{NaSrY}(\text{MoO}_4)_3$, (b) $\text{NaSrY}_{0.8}(\text{MoO}_4)_3:\text{Eu}_{0.2}$, (c) $\text{NaSrY}_{0.7}(\text{MoO}_4)_3:\text{Eu}_{0.1}\text{Yb}_{0.2}$ and (d) $\text{NaSrY}_{0.5}(\text{MoO}_4)_3:\text{Eu}_{0.05}\text{Yb}_{0.45}$ particles excited under 980 nm at room temperature. Only the UC of (d) $\text{NaSrY}_{0.5}(\text{MoO}_4)_3:\text{Eu}_{0.05}\text{Yb}_{0.45}$ particles exhibited a very strong 475-nm emission band in the blue region, and a strong 525-nm and a weak 550-nm emission bands in the green region, while a very weak 650-nm emission band in the red region. The very strong 475-nm emission band in the blue region and the strong 525-nm emission band in the green region correspond to the ${}^7\text{F}_0 \rightarrow {}^5\text{D}_2$ transition and the ${}^7\text{F}_1 \rightarrow {}^5\text{D}_1$ transition, respectively. The weak 550-nm emission band in the green region and the very weak 650-nm emission band in the red region correspond to the ${}^5\text{D}_1 \rightarrow {}^7\text{F}_1$ transition and the ${}^5\text{D}_0 \rightarrow {}^7\text{F}_3$ transition, respectively. The UC of (a) $\text{NaSrY}(\text{MoO}_4)_3$, (b) $\text{NaSrY}_{0.8}(\text{MoO}_4)_3:\text{Eu}_{0.2}$ and (c) $\text{NaSrY}_{0.7}(\text{MoO}_4)_3:\text{Eu}_{0.1}\text{Yb}_{0.2}$ were not detected. The doping amounts of $\text{Eu}^{3+}/\text{Yb}^{3+}$ had a great effect

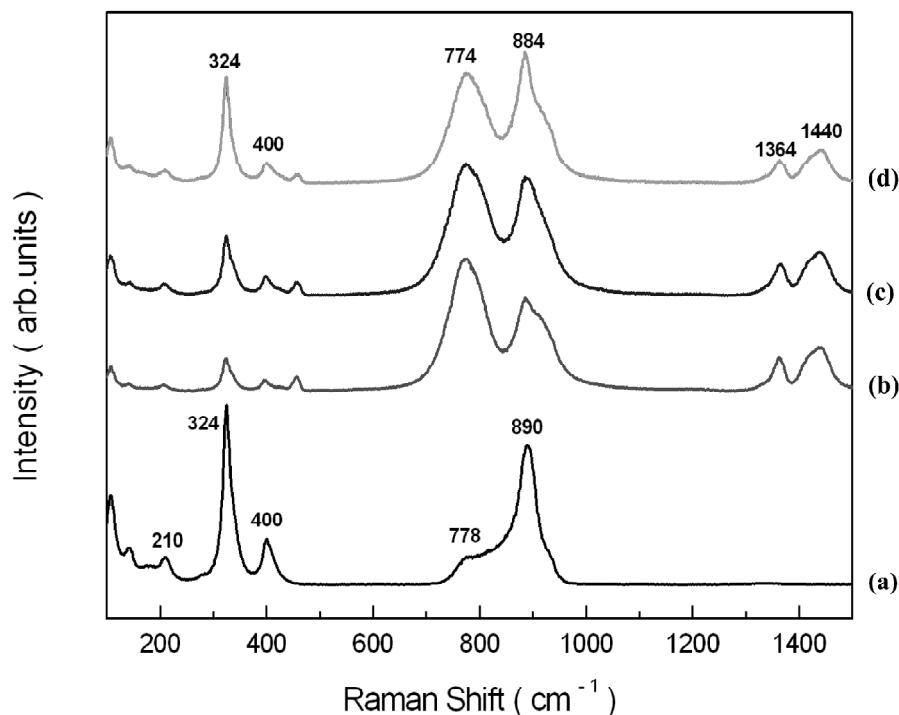


Figure 5: Raman spectra of the synthesized (a) $\text{NaSrY}(\text{MoO}_4)_3$, (b) $\text{NaSrY}_{0.8}(\text{MoO}_4)_3:\text{Eu}_{0.2}$, (c) $\text{NaSrY}_{0.7}(\text{MoO}_4)_3:\text{Eu}_{0.1}\text{Yb}_{0.2}$, and (d) $\text{NaSrY}_{0.5}(\text{MoO}_4)_3:\text{Eu}_{0.05}\text{Yb}_{0.45}$ particles excited by the 514.5-nm line of an Ar ion laser at 0.5 mW.

on the morphological features of the particles and their UC fluorescence intensity. As shown in Fig. 4, the intensity of (d) $\text{NaSrY}_{0.50}(\text{MoO}_4)_3:\text{Eu}_{0.05}\text{Yb}_{0.45}$ is found at $\text{Yb}^{3+}:\text{Eu}^{3+} = 9:1$. Thus, the optimal $\text{Yb}^{3+}:\text{Eu}^{3+}$ ratio is as high as 9:1. Therefore, the higher content of the Yb^{3+} ion used as a sensitizer and lower content of the Eu^{3+} ion for the correct ratio of $\text{Yb}^{3+}:\text{Eu}^{3+}$ (9:1) can remarkably enhance the UC luminescence through the efficient energy transfer [15, 16].

Fig. 5 shows the Raman spectra of the synthesized Raman spectra of the synthesized (a) $\text{NaSrY}(\text{MoO}_4)_3$, (b) $\text{NaSrY}_{0.8}(\text{MoO}_4)_3:\text{Eu}_{0.2}$, (c) $\text{NaSrY}_{0.7}(\text{MoO}_4)_3:\text{Eu}_{0.1}\text{Yb}_{0.2}$, and (d) $\text{NaSrY}_{0.5}(\text{MoO}_4)_3:\text{Eu}_{0.05}\text{Yb}_{0.45}$ particles excited by the 514.5-nm line of an Ar ion laser at 0.5 mW. The internal modes for the (a) $\text{NaSrY}(\text{MoO}_4)_3$ particles were detected at 210, 324, 400, 778 and 890 cm^{-1} , respectively. The well-resolved sharp peaks for the $\text{NaSrY}(\text{MoO}_4)_3$ indicate high crystallinity of the synthesized particles. The internal vibration mode frequencies are dependent on the lattice parameters and the strength of the partially covalent bond between the cation and molecular ionic group MoO_4 . The Raman spectrum of the $\text{NaSrY}(\text{MoO}_4)_3$ crystal in Fig. 5(a) shows the typical molybdate compounds, which is divided into two parts with a wide empty gap of 400-750 cm^{-1} [17-20]. The higher intensity of the wavenumber band at 890 cm^{-1} corresponds to stretching vibrations of the MoO_4 . The stretching vibrations of Mo-O bonds are observed at ~ 778 cm^{-1} . For these stretching vibrations, strong mixing occurs between the Mo-O bonds and the MoO_4 . The bands at

324 and 400 cm^{-1} could be assumed to originate from vibrations of the longer Mo-O bonds, which are employed in the formation of the Mo-Mo bridge. The translational vibration motion of the Sr^{3+} ions is observed at 210 cm^{-1} , whereas the Y^{3+} translations were located below 180 cm^{-1} [21, 22]. The Raman spectra of the doped particles indicate the very strong and dominant peaks at higher frequencies of 774, 884, 1364 and 1440 cm^{-1} and at lower frequencies of 324 and 420 cm^{-1} . These strong disordered peaks at higher and lower frequencies are attributed to the formation of modulated structures of $\text{NaSrY}_{1-x}(\text{MoO}_4)_3$, due to the strong mixing between the Mo-O bonds and the MoO_4 stretching vibrations by the incorporation of the Eu^{3+} and Yb^{3+} elements into the crystal lattice. It should be emphasized that the strongly dominant spectra are attributed to the strong mixing between the Mo-O bonds and the MoO_4 stretching vibrations as well as the concentration quenching effect of Eu^{3+} ions [23, 24].

Conclusion

$\text{NaSrY}_{1-x}(\text{MoO}_4)_3:\text{Eu}^{3+}/\text{Yb}^{3+}$ phosphors with doping concentrations of Eu^{3+} and Yb^{3+} ($x = \text{Eu}^{3+} + \text{Yb}^{3+}$, $\text{Er}^{3+} = 0.05, 0.1, 0.2$ and $\text{Yb}^{3+} = 0.2, 0.45$) were successfully synthesized via the microwave sol-gel route showing a fine and homogeneous morphology with particle sizes of 2-5 μm . Under excitation at 980 nm, only the UC of $\text{NaSrY}_{0.5}(\text{MoO}_4)_3:\text{Eu}_{0.05}\text{Yb}_{0.45}$ particles exhibited a very strong 475-nm emission band in the blue region, and a strong 525-nm and a weak 550-nm emission bands in the green region. The strong 475-nm emission band in the blue region and the strong 525-nm emission band in the green region correspond to the ${}^7\text{F}_0 \rightarrow {}^5\text{D}_2$ transition and the ${}^7\text{F}_1 \rightarrow {}^5\text{D}_1$ transition, respectively. The weak 550-nm emission band in the green region and the very weak 650-nm emission band in the red region correspond to the ${}^5\text{D}_1 \rightarrow {}^7\text{F}_1$ transition and the ${}^5\text{D}_0 \rightarrow {}^7\text{F}_3$ transition, respectively. The Raman spectra of the doped particles indicated the domination of strong peaks at higher frequencies of 774, 884, 1364 and 1440 cm^{-1} and at lower frequencies of 324 and 420 cm^{-1} . The highly modulated structure of the doped samples were attributed to the strong mixing of stretching vibrations between the Mo-O bonds and the MoO_4 as well as the quenching effect of Eu^{3+} concentrations.

Acknowledgement

This research was supported by the Basic Science Research Program through the National Research Foundation of Korea (NRF) funded by the Ministry of Education (2015-058813).

References

- [1] M. Lin, Y. Zho, S. Wang, M. Liu, Z. Duan, Y. Chen, F. Li, F. Xu, T. Lu, *Bio. Adv.*, **30**, 1551 (2012).
- [2] M. Wang, G. Abbineni, A. Clevenger, C. Mao, S. Xu, *Nanomed.*, **7**, 710 (2011).
- [3] A. Shalav, B.S. Richards, M.A. Green, *Sol. Ener. Mater. Sol. Cells*, **91**, 829 (2007).
- [4] C. Guo, H. K. Yang, J.H. Jeong, *J. Lumin.*, **130**, 1390 (2010).
- [5] J. Liao, D. Zhou, B. Yang, R. liu, Q. Zhang, Q. Zhou, *J. Lumin.*, **134**, 533 (2013).
- [6] J. Sun, J. Xian, H. Du, *J. Phys. Chem. Solids*, **72**, 207 (2011).
- [7] T. Li, C. Guo, Y. Wu, L. Li, J.H. Jeong, *J. Alloys Comp.*, **540**, 107 (2012).

- [8] M. Nazarov, D.Y. Noh, *J. Rare Earths*, **28**, 1 (2010).
- [9] J. Sun, W. Zhang, W. Zhang, H. Du, *Mater. Res. Bull.*, **47**, 786 (2012).
- [10] S. Das, A.K. Mukhopadhyay, S. Datta, D. Basu, *Bull. Mater. Sci.*, **32**, 1 (2009).
- [11] T. Thongtem, A. Phuruangrat, S. Thongtem, *J. Nanopart. Res.*, **12**, 2287 (2010).
- [12] C.S. Lim, *Mater. Res. Bull.*, **60**, 537 (2014).
- [13] C.S. Lim, *Infr. Phys. Tech.*, **67**, 371 (2014).
- [14] R. D. Shannon, *Acta Cryst.*, **g**, 751 (1976).
- [15] J. Sun, J. Xian, X. Zhang, H. Du, *J. Rare Earths*, **29**, 32 (2011).
- [16] Q. Sun X. Chen, Z. Liu, F. Wang, Z. Jiang, C. Wang, *J. Alloys Comp.*, **509**, 5336 (2012).
- [17] T.T. Basiev, A.A. Sobel, Y.K. Voronko, P.G. Zverev, *Opt. Mater.*, **15**, 205 (2000).
- [18] V.V. Atuchin, V.G. Grossman, S.V. Adichtchev, N.V. Surovtsev, T.A. Gavrilova, B.G. Bazarov, *Opt. Mater.*, **34**, 812 (2012).
- [19] V.V. Atuchin, A.S. Aleksandrovsy, O.D. Chimitova, A.S. Krylov, M.S. Molokeev, B.G. Bazarov, J.G. Bazarova, Z. Xia, *Opt. Mater.*, **34**, 812 (2012).
- [20] A.A. Savina, V.V. Atuchin, S.F. Solodovnikov, Z.A. Solodovnikova, A.S. Krylov, E.A. Maximovskiy, M.S. Molokeev, A.S. Oreshonkov, A.M. Pugachev, E.G. Khaikina, *J. Solid State Chem.*, **225**, 53 (2015).
- [21] V.V. Atuchin, O.D. Chimitova, T.A. Gavrilova, M.S. Molokeev, Sung-Jin Kim, N.V. Surovtsev, B.G. Bazarov, *J. Cryst. Growth*, **318**, 683 (2011).
- [22] V.V. Atuchin, O.D. Chimitova, S.V. Adichtchev, J.G. bazarov, T.A. Gavrilova, M.S. Molokeev, N.V. Surovtsev, Zh.G. Bazarova, *Mater. Lett.*, **106**, 26 (2013).
- [23] C.S. Lim, A. Aleksandrovsy, M. Molokeev, A. Oreshonkov, V. Atuchin, *J. Solid State Chem.*, **228**, 160 (2015).
- [24] C.S. Lim, *Mater. Res. Bull.*, **48**, 3805 (2013).